Key Engineering Materials
ISSN: 1662-9795, Vol. 821, pp 407-413
doi:10.4028/www.scientific.net/KEM.821.407

Submitted: 2019-05-07
Accepted: 2019-05-23
Online: 2019-09-11

Numerical Simulation of Single Junction InGaN Solar Cell by SCAPS

Mohamed Moustafa[1,a*] and Tariq AlZoubi[2,b]

[1]Department of physics, School of Sciences and Engineering, The American University in Cairo, Egypt

[2]College of Engineering and Technology, American University of the Middle East, Kuwait

[a]mohamed.orabi@aucegypt.edu, [b]Tariq.Alzobi@aum.edu.kw

*corresponding author

Keywords: InGaN, Thin film solar cell, SCAPS

Abstract. The performance of the InGaN single-junction thin film solar cells has been analyzed numerically employing the Solar Cell Capacitance Simulator (SCAPS-1D). The electrical properties and the photovoltaic performance of the InGaN solar cells were studied by changing the doping concentrations and the bandgap energy along with each layer, i.e. n- and p- InGaN layers. The results reveal an optimum efficiency of the InGaN solar cell of ~ 15.32 % at a band gap value of 1.32 eV. It has been observed that lowering the doping concentration N_A leads to an improvement of the short circuit current density (J_{sc}) (34 mA/cm^2 at N_A of 10^{16} cm^{-3}). This might be attributed to the increase of the carrier mobility and hence an enhancement in the minority carrier diffusion length leading to a better collection efficiency. Additionally, the results show that increasing the front layer thickness of the InGaN leads to an increase in the J_{sc} and to the conversion efficiency (η). This has been referred to the increase in the photogenerated current, as well as to the less surface recombination rate.

Introduction

Group III-nitrides are believed to represent an important class of promising semiconductor materials for potential use in several applications such as near-infrared optoelectronics, high speed electronics, and high-efficiency thin film solar cells. Among the ternary compounds, indium gallium nitride (InGaN) alloys have been considered as one of the most important and indispensable materials to be used in the field of the single and multi-junction solar cells and are realized as highly efficient third generation devices. This is due to a batch of rich remarkable semiconducting features as well as their attractive electrical and optical properties. They possess outstanding thermal performance and radiation tolerance, high mobility, along with high absorption coefficient in order of 10^5 cm^{-1} near the band edge, allowing thinner layers of material to absorb most of the solar spectrum [1].

Additionally, one of the most important merit of InGaN alloy is, the so called, the band gap engineering character. One of the approaches through which band gaps with desired properties can be engineered is using what has been termed 'chemical architecture' [2]. A very simple example of this is the use of making ternary, out of binary, compounds in order to achieve a desired band gap, where a wide gap semiconductor and a narrow gap semiconductor are combined to give a substance with a desired intermediate band gap well suitable for a particular application. Indeed, this is the case of $In_xGa_{1-x}N$ where the energy band gap can be tuned continuously, with the indium incorporation (x). The end members of the series i.e. InN and GaN have been reported to possess fundamental energy band gaps of 0.7 eV to 3.42 eV, respectively [3]. This range displays approximately the whole spectrum of the solar energy. Accordingly, varying the bandgap of InGaN alloy offers unique opportunity to design single and multi-junction solar cells. This qualifies them to become promising candidates for band gap engineering, with the flexibility of choosing the number and band gap energies of the constituent junctions, and for the application of the photovoltaic (PV) devices. InGaN solar cells have been investigated by different authors and techniques. For example, InGaN p–i–n and quantum-well solar cells, in which InGaN is treated as

the active layer have been designed as well as the theoretical possibilities of InGaN tandem PV structures [4]. Huang *et al.* demonstrated the nonpolar and semipolar InGaN/GaN multiple-quantum-well (MQW) solar cells grown on the nonpolar m-plane and semipolar plane bulk GaN substrates [6]. Moreover, higher growth rates and lower temperature characterize the InGaN growth using different cost-effective techniques, such as the Metal Organic Chemical Vapor Deposition (MOCVD), Metal Organic Vapor Phase Epitaxy (MOVPE), and Molecular Beam Epitaxy (MBE) [5, 6].

In this paper, we present numerical simulations of InGaN single junction solar cells to provide guidelines for performance improvement through optimization of device structures given achievable material characteristics. The performances of InGaN solar cell that are investigated by SCAPs (Solar Cell Capacitance Simulator) through the calculation of characteristic parameters are: short-circuit current density J_{sc}, open-circuit voltage V_{oc}, the fill factor FF, and conversion efficiency η. These simulations study the effect of indium Content, and thickness of the InGaN absorbing layer. The purpose of this simulation is to obtain the maximum conversion efficiency of InGaN solar cell with the best structure parameters. Additionally, InGaN SJ solar cells are the basic components of the high-efficiency InGaN tandem cells. Hence, the work in this paper is considerable and can pave the way for designing and fabricating InGaN tandem solar cells.

Device Simulation and Analysis

In this numerical study, SCAPS-1D is employed to investigate the InGaN thin film solar cell. SCAPS is a software which has been developed at University of Gent [7]. It is widely used for the simulation of different types of solar cells and the SCAPS simulation results are reported to agree well with the corresponding experimental ones which gives a powerful motivation to use this tool in this work. Most recently, we have employed the SCAPS for the study of others thin film based solar cells e.g. the CdTe solar cells [8, 9]. SCAPS calculates the band diagram in a steady-state, recombination profile, and carrier transport in one dimension using Poisson equation together with hole and electron continuity equations [7]. All the simulations were performed under normalized conditions that are 1000 (W/m^2) light intensity, a temperature of 300 K, and AM1.5 light spectrum illumination.

In this study, we report on the investigation of the performance of single junction InGaN solar cells. Fig. 1 depicts the schematic cross section of a conventional single junction (SJ) InGaN solar cell used in the simulation. The structure studied consists of a p-type emitter and n-type base, with Mo back contact. Incorporating the various material parameters into SCAPS-1D for all of the analysis aspects, solar cell performance parameters such as V_{oc}, J_{sc}, and FF as well as the conversion efficiency η are investigated. The solar cell parameters used in this simulation are available and were obtained and collected in Table 1 [2, 10, 11]. The surface recombination velocities and the reflection coefficients of front and back surfaces are assumed to be 1000 cms^{-1} and 10%, respectively. The ratio of indium content in InGa alloy is denoted as x in $In_xGa_{1-x}N$ material. The mobilities, relative permittivities (ε_r), and effective density of states (DOSs) (N_C and N_V) in the conduction band and the valance band of $In_xGa_{1-x}N$ are taken as the linear interpolations of those of InN and GaN [12].

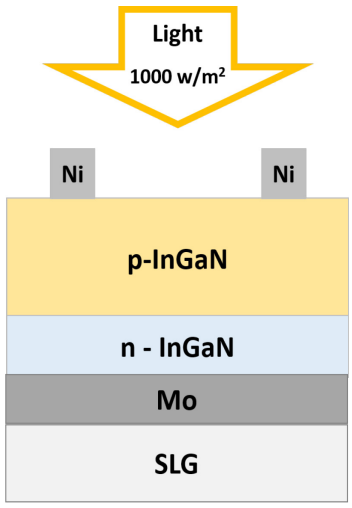

Fig. 1 Schematic diagram of SJ InGaN solar cell.

Table 1 Materials parameters of InGaN used in SCAPS simulations at 300 K.

Parameter	n-InGaN	p-InGaN
Thickness (μm)	0.01 – 0.140	0.03 – 2.1
ε_r	13.1	13.1
$\mu_n\ (cm^2/Vs)$	1000	1000
$\mu_p\ (cm^2/Vs)$	170	170
$N_A\ (cm^{-3})$	10^{16}	10^{16} - 10^{17}
$N_D\ (cm^{-3})$	0	10^{12} - 10^{18}
$E_g\ (eV)$	1.35	1 – 1.8
$N_c\ (cm^{-3})$	1.4×10^{18}	1.4×10^{18}
$N_v\ (cm^{-3})$	4×10^{19}	4×10^{19}
$v_{t-h}(cm/s)$	1×10^{7}	1×10^{7}
$v_{t-e}(cm/s)$	1×10^{7}	1×10^{7}
χ (eV)	5.4	5.5 - 5.1

Results and Discussion

The key application of the $In_xGa_{1-x}N$ material is its tunability band gap energy over a wide range which provides a good spectral match to sunlight. As such, the study here is initiated with the investigation of the band gap effect on the cell performance. The band gap energy and electron affinity have been varied over the ranges from 1 eV to 1.8 eV and from 5.5 to 5.1 eV, respectively. The thicknesses of p-and n-type InGaN were selected to be of 2100 nm and 50 nm, respectively. The doping level of 1×10^{16} cm^{-3} has been used. Fig. 2 depicts the observed conversion efficiency as a function of the band gap of the InGaN solar cell. The results reveal that the performance is optimal at a band gap value of 1.32 eV, with an associated efficiency of 15.32 %. A better approximation for the dependence of the band gap of the InGaN on the indium composition fraction (x) at a temperature of 300 K is is obtained according to Eq. 1 [13]:

$$E_g(In_xGa_{1-x}N) = x.E_g^{InN} + (1-x)\,E_g^{GaN} - b.x.(1-x) \qquad (1)$$

where the band gap energies of InN and GaN are 0.7 eV and 3.42 eV, respectively. x is the indium content and b is the bowing parameter (b = 1.43) [13, 14]. Typically, this approximation is acceptable only if the bowing parameter is smaller than the band gaps of the constituent materials. Apllying Eq. 1, the obtained value of the band gap associated with the optimal efficiency is found to be at x= 0.64. These results compare well with some previous studies of $In_xGa_{1-x}N$ single junction solar cell where the In content of the InGaN layers has been defined with x =0.622 for achieving the limit-efficiency of the single junction SJ solar cell [15].

The doping concentration of both p-type and n-type InGaN layers has reported an influence on the number of the photogenerated carriers which accordingly has a consequence on the short circuit current density J_{sc}, the open circuit voltage, the maximal power, as well as the conversion efficiency of the solar cell. To study this effect, the acceptor doping concentration N_A has been varied from 1×10^{16} cm^{-3} to 1×10^{17} cm^{-3}. As shown in Fig. 3, an improvement of the J_{sc} is observed when the acceptor doping concentration NA decreases. J_{sc} is found to reach 34 mA/cm^2 at N_A of 10^{16} cm^{-3}.

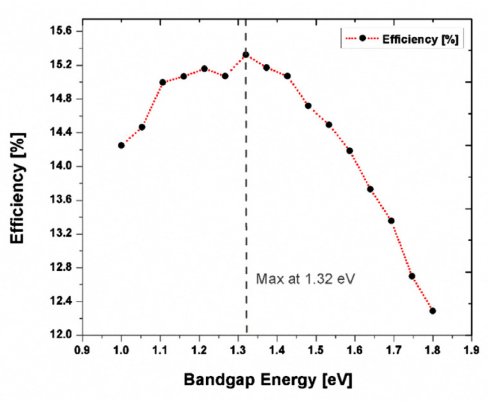

Fig. 2 The conversion efficiency of InGaN SJ solar cell as a function of the band gap.

The observed behavior can be most attributed to the increase of the carrier mobility and hence the increase in the minority carrier lifetime with the decrease of the doping concentration N_i (i = A or D). This leads to an enhancement in the minority carrier diffusion length and better collection efficiency, which affects the J_{sc} directly, resulting in the improvement of the J_{sc}. The minority carrier diffusion length L increased ultimately with decreasing doping concentration. So, J_{sc} increased with the decrease of the doping concentration. If the carrier mobility model of InGaN is assumed to be similar to GaN, carrier mobility can be calculated by Eq. 2

$$\mu_i(N) = \mu_{min,i} + \frac{\mu_{max,i} - \mu_{min,i}}{1+(N/N_{g,i})^{\gamma_i}} \tag{2}$$

where i = n, p for electrons and holes, respectively, and N is the doping concentration, while the model parameters $\mu_{max,i}$, $\mu_{min,i}$ (in $cm^2V^{-1}s^{-1}$), $N_{g,i}$ (in cm^{-3}) and γ_i (1.0 for electrons an 2.0 for holes) depending on the type of semiconductor material. Additionally, The minority carrier diffusion length L is given by $L = \sqrt{D\,\tau}$, where τ was the minority carrier lifetime and D the minority carrier diffusivity. The Einstein relation is given by

$$D = \left(\frac{k_B T}{q}\right)\mu \tag{3}$$

From Eqs. 2, and 3, it could be seen that L increased ultimately with decreasing the doping concentration. So, J_{sc} increased when the doping concentration was decreased as seen in Fig. 3. In regards to the V_{oc}, a decrease of the V_{oc} is observed with decreasing the doping level (see Fig. 3). It reaches 0.47 eV at 1×10^{16} cm^{-3} N_A. The V_{oc} of a p–n junction solar cell and the reverse saturation current density are given by Eq. (4) and Eq. (5), respectively [17].

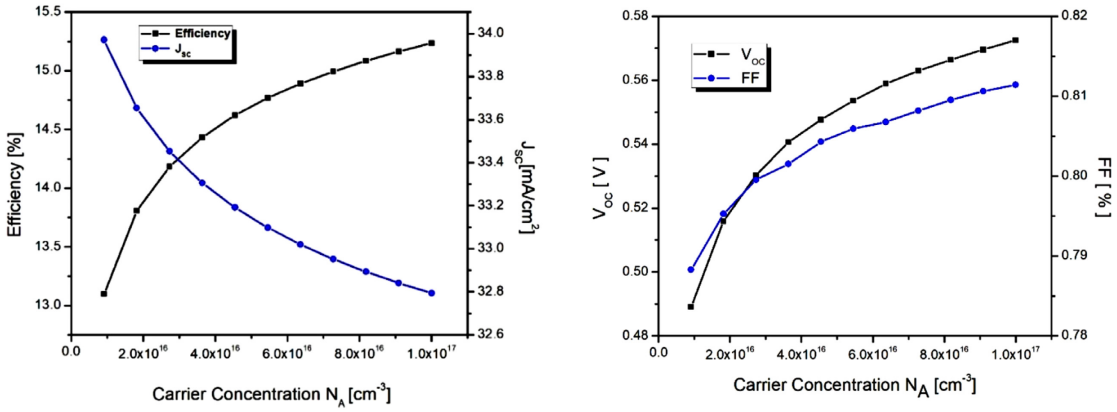

Fig. 3 Parameters of the InGaN solar cell as a function of the N_A. Left: Conversion efficiency (black squares) and J_{sc} (blue dots). Right: V_{oc} (black squares) and FF (blue dots).

$$V_{oc} = \frac{k_B T}{q}\ln\left(\frac{J_{sc}}{J_0} + 1\right) \tag{4}$$

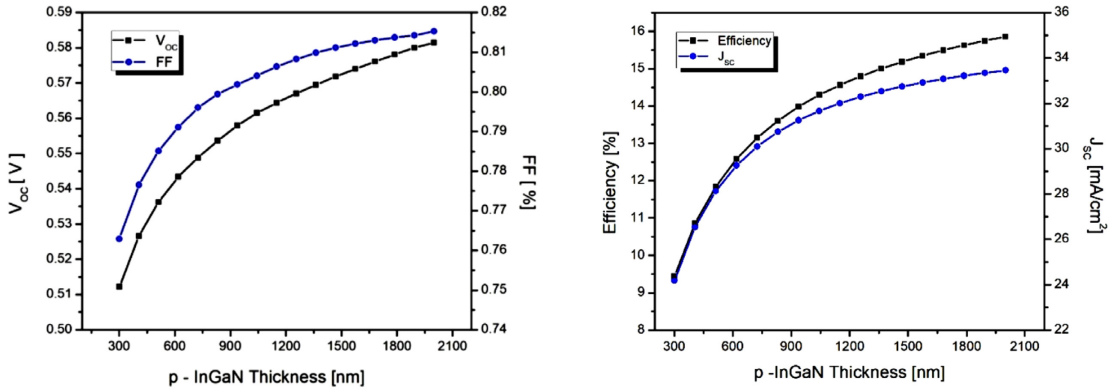

Fig. 4 Performance parameters of the InGaN cell as a function of the p-InGaN thickness. Left: V_{oc} (black squares) and FF (blue dots). Right: efficiency (black squares) and J_{sc} (blue dots).

$$J_0 = qn_i^2 . \frac{L_n}{\tau_n N_A} \left(\frac{(S_n \tau_n / L_n) \cosh(x_j/L_n) + \sinh(x_j/L_n)}{(S_n \tau_n / L_n) \sinh(x_j/L_n) + \cosh(x_j/L_n)} \right) qn_i^2 . \frac{L_p}{\tau_p N_D} \left(\frac{(S_p \tau_p / L_p) \cosh(H/L_p) + \sinh(H/L_p)}{(S_p \tau_p / L_p) \cosh(H/L_p) + \sinh(H/L_p)} \right) \quad (5)$$

Where n_i is the intrinsic carrier concentration, J_n and J_p are the photocurrent densities due to electrons and holes collected, respectively, at the depletion edges x_j and x_j+W. $L_{n,h}$, $S_{n,h}$, and $\tau_{n,h}$ are the minority carrier diffusion length, surface recombination velocity, and lifetime, respectively. x_j, W and H are the junction depth, the depletion region width, and the neutral thicknesses of the n-type region, respectively. According to Eqs. (4) and (5), the reverse saturation current density decreases with the increasing of the doping concentration, inducing the increase of the V_{oc}. Furthermore, the optimum efficiency of InGaN single-junction solar cell reached 15.32 % when the acceptor doping concentration was 1×10^{17} cm^{-3}.

The layer thickness plays an important role in determining the J_{sc}. It is well understood that, thin InGaN absorber will result in an incomplete light absorption. On the other hand, if the InGaN absorber is grown too thick, the quality of the InGaN layer and the collection efficiency is degraded, resulting in poor photovoltaic performance. The results show in Fig. 4 that, increasing the front

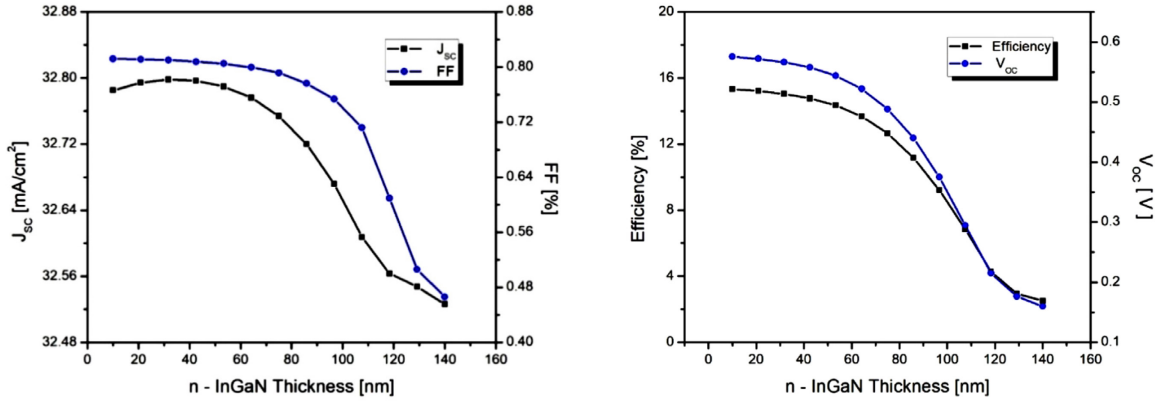

Fig. 5 Performance parameters of the InGaN solar cell as a function of the n-InGaN thickness. Left: J_{sc} (black squares) and FF (blue dots). Right: η (black squares) and V_{oc} (blue dots).

layer thickness of the active region InGaN leads to an increase in the J_{sc} and the conversion efficiency (η). As the thickness of the InGaN layer increases, more photons would be absorbed, especially in an energy range of $E_{(InGaN)} \leq E_{Photon} \leq E_{(GaN)}$. This results in an increase in the photogenerated current, which accordingly enhances the photogeneration rate. This is mainly attributed to the enhanced absorption of the incident light due to the thickness of the absorber layer. At the same time, taking the surface recombination parameter into account, the η of the depletion

region will be improved with the increase of the thickness as this last is not close to the surface. In contrary to this discussion, when the front layer thickness increases, the distance between the space charge region and the surface increases, which reduces the collection efficiency inducing a reduction of the J_{sc}. However, since the effective collection efficiency is the product of the η and the photogeneration rate, when both parameters are taken into consideration we found the J_{sc} increases with increasing the thickness as shown in Fig. 4. The obtained results from the simulation reveal that the effect of the two parameters, i.e. the surface recombination and the absorption factor, are considered to be of dominant effect. The increase of the collection efficiency leads to the increase of the J_{sc} and the conversion efficiency as observed in the Fig. 4.

Fig. 5 shows the electrical and performance parameters of the InGaN solar cell as a function of the n-type thickness. The overall performance of the solar cell with the parameters is enhanced with the decrease of the n-layer thickness. The parameters are almost constant with slight reduction up to a thickness of 50 nm where a dramatic reduction is observed when the thickness is increased above 70 nm. The optimal J_{sc} is observed to increase to 32.8 mA/m^2 and the efficieny of 15.32 % and the V_{oc} is of 0.57 eV. It has been observed that the conversion efficiency is enhanced with the decrease of the back layer thickness until 50 nm, however, beyond this value it remains almost constant. The reduction of the efficiency might be primarily attributed to the large absorption coefficient in the direct band gap InGaN alloys. This causes the majority of the electron-hole pairs to be less generated than a diffusion length away from the junction. So, for short carrier lifetimes, the carriers recombine quickly which consequently implies a reduction in the conversion efficiency [20]. Additionally, a thinner layer leads to a thinner space charge region whcih in turns might mediates the junction to near ohmic rather than schottky one. It is also noteworthy to mention here that, the reduction (weakness performance of thicker layers) might be attributed to the possibility of the effect of the created shunt resistance accompanied with the thicker layer, which can be observed from the low V_{oc} value (~ 0.15 eV). Therefore, it can be conculded that the electrical parameters of the InGaN solar cell are less affected by the back layer thickness than the front layer thickness. From the obtained results, we can say that the thickness of the n-type should be kept not greater than 50 nm in order to maintain well performance of the solar cell.

Summary

The photovoltaic performance of p-InGaN/n-InGaN single junction solar cells has been numerically investigated. The simulation is conducted using the solar cell capacitance simulator (SCAPS) software. An optimal conversion efficiency of 15.32 % has been reported at a band gap of 1.32 eV which corrresponds to 64 % of the Indium compositions. Additionally, the obtained results show that J_{sc}, V_{oc}, and the conversion efficiency depend on the dopping level as well as the layers thickness. Increasing the doping concentration N_A leads to an improvement of the J_{sc}. A value of 34 mA/cm^2 at N_A of 10^{16} cm^{-3} has been obtained. This trend is attributed to the increase of the carrier mobility and enhancement in the minority carrier diffusion length. Finally, the thickness of the p-layer active layer has been found to play a role on the overall cell perormance due to dominant effects, namely the photogeneration rate and the surface recombination.

References

[1] L. A. Vilbois, A. Cheknane, A. Bensaoula, C. Boney, and T. Benouaz, Simulation of a solar cell based on InGaN, Energy Procedia 18 (2012) 795-806.

[2] M. Moustafa, A. Paulheim, M. Mohamed, C. Janowitz, R. Manzke, Angle-resolved photoemission studies of the valence bands of ZrS_xSe_{2-x}, Appl. Surf. Sci. 366 (2018) 397-403.

[3] H. Xiao, X. Wang, J. Wang, N. Zhang, H. Liu, Y. Zeng, J. Li, and Z. Wang, Growth and characterization of InN on sapphire substrate by RF-MBE, J. Cryst. Growth 276 (2005) 401

[4] H. Hamzaoui, A.S. Bouazzi, and B. Rezig, Theoretical possibilities of $In_xGa_{1-x}N$ tandem PV structures, Sol. Energy Mater. Sol. Cells 87 (2005) 595-603.

[5] X. Huang, Houqiang Fu, H. Chen, X. Zhang, Z. Lu, J. Montes, M. Iza, St. P. DenBaars, S. Nakamura, and Y. Zhao, Nonpolar and semipolar InGaN/GaN multiple-quantum-well solar cells with improved carrier collection efficiency, Appl. Phys. Lett. 110, (2017) 161105

[6] Z. Keyan, W. Yadong, and C. Soo Jin, Low dimensional nanostructured InGaN multi-quantum wells by selective area heteroepitaxy, Phys. Status Solidi C, 6 S2S (2009) S514-S518.

[7] M. Burgelman, K. Decock, S. Khelifi and A. Abass, Advanced electrical simulation of thin film solar cells, Thin Solid Films 535 (2013) 296-301.

[8] M. Moustafa and T. AlZoubi, Numerical study of CdTe solar cells with p-$MoTe_2$ TMDC as an interfacial layer using SCAPS, Modern Physics Letters B 32, No. 23, (2018) 1850269

[9] M. Moustafa and T. AlZoubi, Effect of the n-$MoTe_2$ interfacial layer in cadmium telluride solar cells using SCAPS, Optik 120 (2018) 101-105.

[10] A. S. Barker, Jr. and M. Ilegems, Infrared Lattice Vibrations and Free-Electron Dispersion in GaN, Phys. Rev. B 7 (1973) 743.

[11] Z. Z. Bandić, P. M. Bridger, E. C. Piquette, and T. C. McGill, Minority carrier diffusion length and lifetime in GaN, Appl. Phys. Lett. 72 (1998) 3166.

[12] X. Huang, Houqiang Fu, H. Chen, X. Zhang, Z. Lu, J. Montes, M. Iza, St.P. DenBaars, S. Nakamura, and Y. Zhao, Nonpolar and semipolar InGaN/GaN multiple-quantum-well solar cells with improved carrier collection efficiency, Appl. Phys. Lett. 110 (2017) 161105

[13] J.A. Van Vechten, T. K. Bergstresser, Electronic Structures of Semiconductor Alloys, Phys. Rev. B1 (1970) 3351.

[14] F. Bouzid and L. Hamlaoui, Investigation of InGaN/Si double junction tandem solar cells, J. Fundam Appl Sci. 4 (2012) 59-71.

[15] A. Mesrane, F. Rahmoune, A. Mahrane, and A. Oulebsir, Design and Simulation of InGaN p-n Junction Solar Cell, Int. J. photoenergy 2015 (2015) 1-9.

[16] S. R. Kurtz, P. Faine, and J. M. Olson, Modeling of two-junction, series-connected tandem solar cells using top-cell thickness as an adjustable parameter, J. Appl. Phys. 68 (4) (1990) 1890-895.

[17] Z. Li, H. Xiao, X. Wang, C. Wang, Q. Deng, L. Jing, J. Ding, X. Hou, Theoretical simulations of InGaN/Si mechanically stacked two-junction solar cell, Physica B 414 (2013) 110-114.